J Bioenerg Biomembr (2011) 43:447–455
DOI 10.1007/s10863-011-9379-y

Structural elements of the C-terminal domain of subunit E ($E_{133-222}$) from the *Saccharomyces cerevisiae* V_1V_O ATPase determined by solution NMR spectroscopy

Sankaranarayanan Rishikesan · Gerhard Grüber

Received: 17 June 2011 / Accepted: 15 July 2011 / Published online: 9 August 2011

Abstract Subunit E of the vacuolar ATPase (V-ATPase) contains an N-terminal extended α helix (Rishikesan et al. J Bioenerg Biomembr 43:187–193, 2011) and a globular C-terminal part that is predicted to consist of a mixture of α-helices and β-sheets (Grüber et al. Biochem Biophys Res Comm 298:383–391, 2002). Here we describe the production, purification and 2D structure of the C-terminal segment $E_{133-222}$ of subunit E from *Saccharamyces cerevisiae* V-ATPase in solution based on the secondary structure calculation from NMR spectroscopy studies. $E_{133-222}$ consists of four β-strands, formed by the amino acids from K136-V139, E170-V173, G186-V189, D195-E198 and two α-helices, composed of the residues from R144-A164 and T202-I218. The sheets and helices are arranged as β1:α1:β2:β3:β4:α2, which are connected by flexible loop regions. These new structural details of subunit E are discussed in the light of the structural arrangements of this subunit inside the V_1- and V_1V_O ATPase.

Keywords V_1V_O ATPase · V-ATPase · Subunit E · Vma4p · *Saccharomyces cerevisiae* · NMR spectroscopy

Abbreviations

DTT	Dithiothreitol
EDTA	Ethylenediaminetetraacetic acid
IPTG	Isopropyl-β-D-thio-galactoside
PMSF	Phenylmethylsulfonyl fluoride
Pefabloc	4-(2-Aminoethyl)-benzenesulfonyl fluoride hydrochloride
NMR	Nuclear magnetic resonance
NOE	Nuclear Overhauser effect
NTA	Nitrilotriacetic acid
PAGE	Polyacrylamide gel electrophoresis
PCR	Polymerase chain reaction
RMSD	Root mean square deviation
SDS	Sodium dodecyl sulfate
Tris	Tris-(hydroxymethyl) aminomethane

Introduction

Eukaryotic vacuolar ATPases (V-ATPases) are ATP-driven proton pumps that acidify the organelles and are essential for the vesicular trafficking in eukaryotic cells. Defects of cell trafficking in the biological system have been reported in numerous human diseases like cancer, neurological disorders, autoimmune and metabolic diseases including diabetes (Marshansky and Futai 2008). V_1V_O ATPases are large multi-subunit complexes that are organized in the two distinct sectors, V_1 and V_O. The V_1 domain is composed of eight subunits, A-H, in a proposed stoichiometry of A_3:B_3:C:D:E_{2-3}:F:G_{2-3}:H_X. The membrane-integrated V_O domain consists of five subunits *a*, *c*, *c′*, *c″*, *d* and *e*, which pumps protons via the membrane in an ATP-driven process (Grüber and Marshanski 2008). Electron micrographic image analysis of V_1 ATPase from *Manduca sexta* reveals the existance of a headpeice with six elongated catalytic subunits, A_3 and B_3, arranged alternatively along with a

Electronic supplementary material The online version of this article (doi:10.1007/s10863-011-9379-y) contains supplementary material, which is available to authorized users.

S. Rishikesan · G. Grüber (✉)
School of Biological Sciences, Nanyang Technological University,
60 Nanyang Drive,
Singapore 637551, Republic of Singapore
e-mail: ggrueber@ntu.edu.sg

central cavity (Radermacher et al. 2001). The A_3B_3-hexamer embeds the catalytic centers, in which ATP-hydrolysis takes place. In the V_1 ATPase a central stalk, constituting of C-H, protrudes at the bottom of the A_3B_3 (Radermacher et al. 2001; Chaban et al. 2005). By comparison, in the entire V_1V_O ATPases the A_3B_3-headpiece is connected to the V_O sector via a central and two peripheral stalks as shown for the *Saccharomyces cerevisiae* enzyme (Wilkens et al. 1999; Diepholz et al. 2008), formed by the subunits C to H, and indicating a structural rearrangement of these stalk subunits during assembly and disassembly of the V_1 and V_O sector (Grüber 2003).

Structural insight in the stalk subunits of the *S. cerevisiae* V_1V_O ATPase started with the crystal structure of subunit H, which is characterized by a large α-helical N-terminal domain, a shallow groove and a C-terminal domain connected by a four-residue loop (Sagermann et al. 2001). Subunit C is formed by an upper head domain, a large globular foot and an elongated neck domain (Drory et al. 2004; Armbrüster et al. 2004). A low resolution solution structure of the recombinant subunit F from *S. cerevisiae* V-ATPase revealed two distinct domains, an egg-like domain and a hook-like segment, which allows the coupling of hydrolysis with H^+-pumping (Basak et al. 2011). NMR spectroscopy data revealed that subunit G forms an elongated and highly α-helical structure (Rishikesan et al. 2009, 2010). Similarly, the *S. cerevisiae* V-ATPase subunit E has been described as an elongated protein, forming together with the recombinant subunit G a long rod shaped structure of 180 Å with distinct thick and narrow extremeties (Diepholz et al. 2008). The narrow end is formed by the N-terminal α-helices of subunit G and E, whose structures have been solved by NMR spectroscopy (Rishikesan et al. 2010, 2011). The thick shape of the E-G is proposed to be contributed by the α-helical C-terminus of subunit G (Rishikesan et al. 2010) and the predicted globular C-terminal domain of subunit E (Grüber et al. 2002; Jones et al. 2005).

Subunit E (Vma4p) of the *S. cerevisiae* V_1V_O ATPase is an essential component of the V_1 assembly, as disruption of the gene on the yeast (Vma4) resulted in a disassembly of the V_1V_O complex (Kane and Smardon 2003). The protein has shown to be in a close proximity to the nucleotide-binding subunits A, B (Xu et al. 1999; Arata et al. 2002; Rizzo et al. 2003; Owegi et al. 2005) and the coupling subunit D in the V_1 ATPase (in a nucleotide dependent manner (Grüber et al. 2000)). Mutational analysis has demonstrated communication between subunit E and catalytic sites at the A_3B_3 hexamer, suggesting potential regulatory roles for the carboxyl end of subunit E (Owegi et al. 2005). Crosslink formation of E and B (Arata et al. 2002) as well as the use of a Flag-tag at the C-terminus of subunit E in electron micrographs of *S. cerevisiae* V_1V_O ATPase supported the localization of the very C-terminal region of E in the neighborhood of the major subunits A and B (Diepholz et al. 2008). Because of the critical role of the C-terminal region of E with the catalytic headpiece in the assembly and its participation in the regulation of the enzyme, we aimed to get a deeper insight into this segment. Therefore, we produced and purified a highly pure and mono-dispersed recombinant C-terminal region of subunit E ($E_{133-222}$) from *S. cerevisiae* V-ATPase. NMR spectroscopy has been used to determine the first two-dimensional structure of this domain in solution.

Materials and methods

Biochemicals

ProofStart™ DNA Polymerase and Ni^{2+}-NTA-chromatography resin were received from Qiagen (Hilden, Germany); restriction enzymes were purchased from Fermentas (St. Leon-Rot, Germany). Chemicals for gel electrophoresis were received from Serva (Heidelberg, Germany). ($^{15}NH_4$)Cl and (^{13}C) glucose were purchased from Cambridge Isotope Laboratories (Andover, U.S.A.). All other chemicals were at least of analytical grade and received from BIOMOL (Hamburg, Germany), Merck (Darmstadt, Germany), Sigma (Deisenhofen, Germany) or Serva (Heidelberg, Germany).

Cloning and purification of recombinant $E_{133-222}$

$E_{133-222}$ was cloned from the *S. cerevisiae* genome through PCR cloning method using 5′-TTT-CCA-TGG-TGT-TGG-AAC-CTA-AGG-CGA-TTG-3′ as forward primer and 5′-TTG-AGC-TCT-CAC-AAT-TCC-AAT-CTG-ATG-GCG-3′ as reverse primer. PCR products were incorporated with *NcoI* and *SacI* restriction sites and were ligated to the pET9d1(+)-His_3 vector (Grüber et al. 2002). The uniformly ^{15}N- and $^{15}N/^{13}C$- labeled $E_{133-222}$ was expressed in *Escherichia coli* BL21 (DE3) cells using M9 minimal media containing $^{15}NH_4Cl$, or $^{15}NH_4Cl$ plus [U-^{13}C]-glucose. The recombinant protein was induced by the addition of isopropyl-β-D-thio-galactoside (IPTG) to the culture. Cells were harvested at 8,000× *g* for 15 min at 4 °C and lysed on ice by sonication in the buffer containing 50 mM HEPES, pH 7.0, 150 mM NaCl, 1 mM DTT, 2 mM Pefabloc^{Sc} and 2 mM phenylmethylsulfonyl fluoride (PMSF). The lysate was cleared by centrifugation at 10,000× *g* for 30 min at 4 °C, the supernatant was passed through a filter (0.45 mm pore-size) and supplemented with Ni^{2+}-NTA resin. The N-terminal His-tagged protein, (MKHHH-$E_{133-222}$), was allowed to bind to the matrix for 2 h at 4 °C by mixing on a sample rotator (Neolab), and eluted with an imidazole-gradient (25–200 mM) in the

buffer described above. Fractions containing His-tagged proteins were identified by SDS-PAGE (Laemmli 1970), pooled and concentrated using Centriprep YM-3 (3 kDa molecular mass cut-off) spin concentrators (Millipore) and subsequently applied on a size exclusion column Superdex HR75 (10/30, GE Healthcare). Selected fractions were concentrated in 3 kDa cut-off centricon. The purity of the protein sample was analysed by SDS-PAGE, which were stained with Coomassie Brilliant Blue R250. Protein concentrations were determined by the bicinchoninic acid assay (BCA; Pierce, Rockford, IL, USA).

Secondary structure determination of *S. cerevisiae* $E_{133\text{-}222}$ using CD spectroscopy

Steady state CD spectra of $E_{133\text{-}222}$ were measured in the far UV-light (190–260 nm) using a CHIRASCAN spectrometer (Applied Photophysics). Spectra were collected in a 60 µl quartz cell (Hellma) with a path length of 0.1 mm, at 20 °C at a step resolution of 1 nm. The readings were average of 2 s at each wavelength and the recorded milli-degree values were the average of three determinations for the sample. The CD spectrum was acquired in a buffer of 25 mM phosphate (pH 6.8), 200 mM NaCl and 5 mM EDTA with a protein concentration of 2.0 mg/ml. The spectrum of the buffer was subtracted from the spectrum of $E_{133\text{-}222}$. CD values were converted to mean residue molar ellipticity (θ) in units of deg $\times$ cm^2 $\times$ $dmol^{-1}$ $\times$ aa^{-1} using the software *Chirascan Version 1.2*, Applied Photophysics. This baseline corrected spectrum was used as input for computer methods to obtain predictions of secondary structure.

NMR data collection and processing

The NMR sample of $E_{133\text{-}222}$ (1 mM) was prepared in 90% H_2O and 10% D_2O containing 25 mM NaH_2PO_4 (pH 6.8),

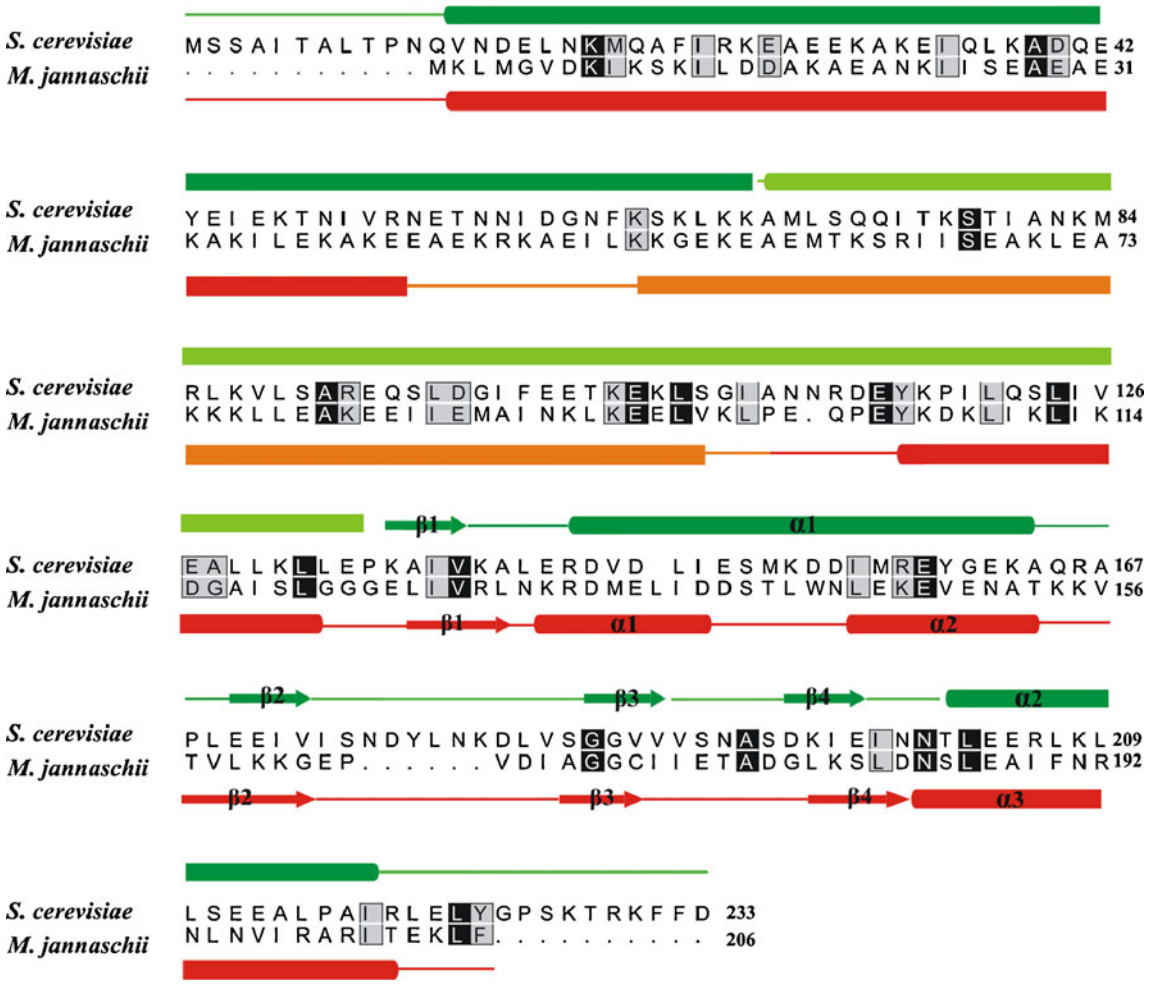

Fig. 1 Multiple sequence alignment of subunit E of *S. cerevisiae* V-ATPase with subunit E of A_1A_O ATP synthase from *M. jannaschii*. The secondary structures of $E_{1\text{-}69}$ (Rishikesan et al. 2011) and the presented $E_{133\text{-}222}$ from *S. cerevisiae* V-ATPase are shown in green and were determined by NMR spectroscopy. The uncharacterized region, which is predicted to be α-helical, is presented in light green. In comparison, the secondary structure for the segments $E_{1\text{-}52}$ (Gayen et al. 2009) and $E_{101\text{-}206}$ (Balakrishna et al. 2010), determined by NMR and crystallography, respectively, are shown in red. The orange region reveals the predicted α-helical segment

200 mM NaCl and 5 mM EDTA. These conditions were used after optimizing the ^{15}N HSQC spectrum based on different temperature and different NaCl concentration on the buffer. All the NMR experiments were performed at 293 K on a Bruker Avance 600 MHz spectrometer. The experiments recorded on $^{15}N/^{13}C$-labelled sample were HNCO, CBCA(CO)NH, HNCACB and 3D ^{15}N-NOESY-HSQC. The 3D ^{15}N-NOESY-HSQC was recorded using mixing time of 200 ms. All the two- and three-dimensional experiments made use of pulsed-field gradients for coherence selection and artifact suppression, and utilized gradient sensitivity enhancement schemes. Quadrature detection in the indirectly detected dimensions was achieved using either the States/TPPI (time-proportional phase incrementation) (Marion et al. 1989) or the echo/anti-echo method (Bax et al. 1980; Claridge 1999). Baseline corrections were applied wherever necessary. The proton chemical shift was referenced to the methyl signal of DSS (2, 2-dimethyl-2-silapentane-5-sulphonate Cambridge Isotope Laboratories) as an external reference to 0 ppm. The ^{13}C and ^{15}N chemical shifts were referenced indirectly to DSS. All the NMR data were processed using Bruker Avance spectrometer in-built software Topspin 2.1 version. Peak-picking and data analysis of the Fourier transformed spectra were performed with the SPARKY program (Kneller and Goddard 1997).

Structure calculation of $E_{133\text{-}222}$ based on NMR-data

The structure calculation was performed from the first methionine after the His-tag exclusion at the N-terminus of $E_{133\text{-}222}$, which are essentially unstructured. The sequential assignments were achieved using triple-resonance backbone experiments (HNCO, CBCA(CO)NH and HNCACB) and all the side chain assignments were done using the (H) CCCONH experiments.

Results and discussion

Production and purification of recombinant $E_{133\text{-}222}$

The *S. cerevisiae* V-ATPase subunit E forms an N-terminal extended α-helix in solution (Rishikesan et al. 2011) and is proposed to consist of a globular C-terminal segment of α-helical and β-sheet, which are made up by the amino acids 135 to 233 (Fig. 1). To avoid the predicted flexible structure of the very C-terminal sequence 223–239 of subunit E, we successfully amplified DNA, encoding for the C-terminal region of amino acids 133–222, called $E_{133\text{-}222}$. The amplified DNA was cloned into the bacterial vector pET9d-His_3 (Grüber et al. 2002). The recombinant *S. cerevisiae* $E_{133\text{-}222}$ with an apparent molecular mass of 10.3 kDa was produced in high amounts and found within the soluble fractions. A Ni^{2+}-NTA resin column and an imidazole-gradient (25–200 mM) in 50 mM HEPES, pH 7.0, 150 mM NaCl, 1 mM DTT, 2 mM Pefabloc^{SC} and 2 mM PMSF was used to purify the protein. The elution fractions from the Ni^{2+}-NTA purification containing the $E_{133\text{-}222}$ were collected and applied on to a size exclusion column (Fig. 2a). Analysis of the isolated protein by SDS-PAGE revealed a high purity of $E_{133\text{-}222}$ (Fig. 2a). Circular dichroism spectroscopy has been used to collect spectra in the range of 190 to 260 nm and to determine the secondary structural content of the protein. The overall spectrum is a typical characteristic of the presence of α-helical and β-sheeted structures in the protein (Fig. 2b) with a content of 44% α-helix, 21% β-sheet and 38% random coil. These results are concurrent with the data analysis of recombinant subunit E (Vma4) which exhibited 32% α-helix and 23% β-sheet (Grüber et al. 2002). Since the solution structure of the N-terminus of subunit E ($E_{1\text{-}69}$) showed an extended helix (Rishikesan et al. 2011), the presented data confirm, that the C-terminal segment is a formed by an α-helical and β-sheet structure.

Resonance assignment and 2-D structure of $E_{133\text{-}222}$

Like for the CD measurements, buffer exchange of $E_{133\text{-}222}$ from HEPES to 25 mM NaH_2PO_4 (pH 6.0), 200 mM NaCl and 5 mM EDTA has been done, prior to

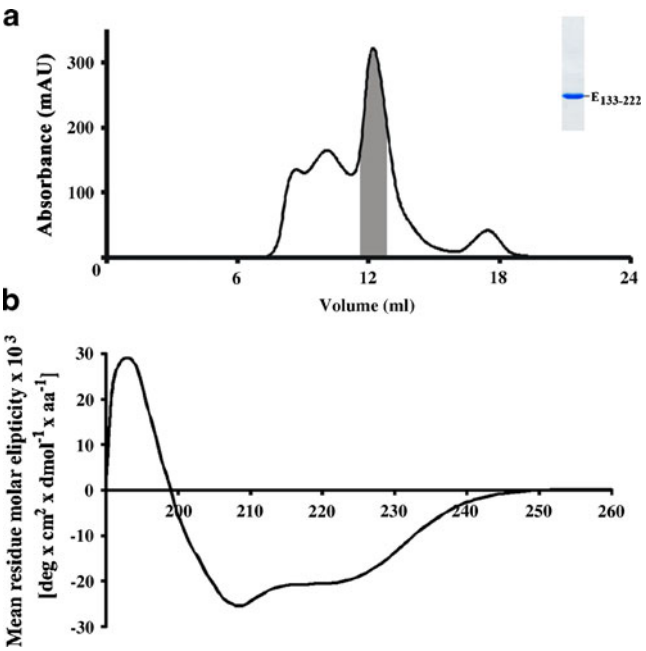

Fig. 2 **a** Elution profile of $E_{133\text{-}222}$ from the size exclusion column, Superdex HR75, against buffer containing 50 mM HEPES, pH 7.0, 150 mM NaCl, 1 mM DTT, 2 mM Pefabloc^{Sc} and 2 mM PMSF. SDS gel insert on the top right corner shows the final purified recombinant $E_{133\text{-}222}$ of the *S. cerevisiae* V-ATPase. **b** Far UV-CD spectrum of $E_{133\text{-}222}$

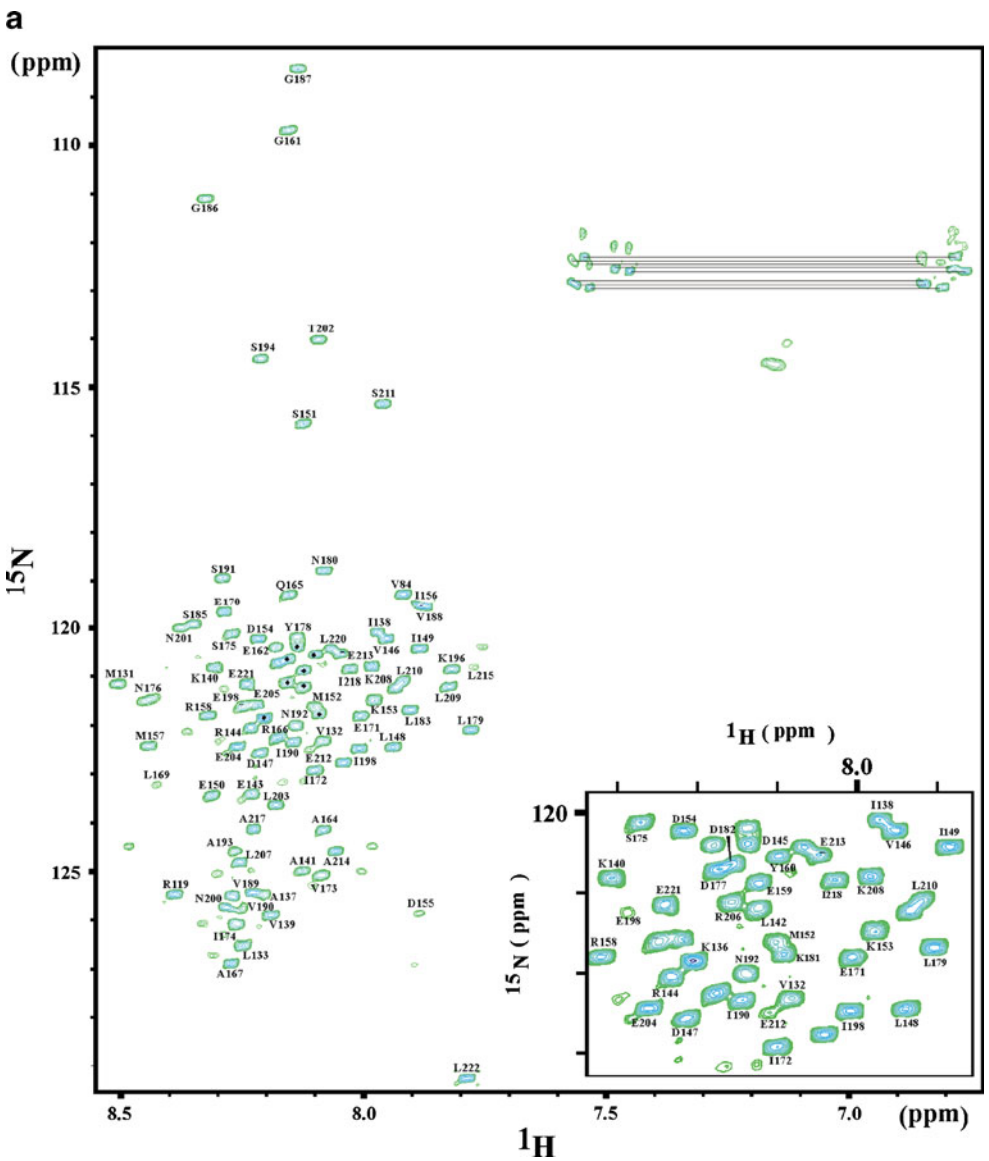

Fig. 3 **a** 2D ^{1}H-^{15}N-HSQC spectrum of *S. cerevisiae* $E_{133-222}$ (1 mM) in 25 mM sodium phosphate buffer (6.0), 200 mM NaCl and 5 mM EDTA at 293 K. Signals from the side-chain NH_2 groups are connected by horizontal lines. **b** Chemical shift index (CSI) plot of $E_{133-222}$ derived from ΔCα-ΔCβ, where '+1' represents α-helical tendency, while '-1' represents the β-strand tendency (Wishardt et al. 1992). **c** Topological model based on the determined secondary structure of $E_{133-222}$, as per CSI, where the yellow color represents the respective four β-strands and green color represents the two respective α-helices

NMR spectroscopy experiments. The ^{1}H ^{15}N HSQC spectrum of $E_{133-222}$ appeared to be properly folded and the peaks are well dispersed, and most of the individual peaks are distinguished (Fig. 3a). 92 amino acid residues were observed in the $^{15}N/^{1}H$ HSQC spectrum except E134, R158 and D195, excluding the three proline at P135, P168 and P216. The chemical shifts on the NH plane were dispersed to ~2.0 ppm for the amide proton resonance and this predominantly indicates the presence of a mixed population of helix and sheeted conformation. The comprehensive ^{15}N, ^{13}C and ^{1}H resonance assignments obtained for the $E_{133-222}$ peptide have been deposited at the BioMagResBank (BMRB) database (Accession number 17766).

The sequential assignments of the $E_{133-222}$ were performed using the ^{15}N and/or ^{13}C signals of the double and triple resonance backbone experiments on a combined analysis of the triple resonance spectrum HNCACB versus CBCA(CO)NH and HNCAO versus HNCO spectra. Overall, the limited chemical shift dispersion of ~2.0 ppm for the amide proton resonance indicates a predominantly mixed population of α-helix and β-sheets on the protein. 85 amino acids possessed the respective α-, β- and carbonyl peaks except the above mentioned seven residues, which include three proline residues as well. Most of the cross peaks in the ^{1}H-^{15}N HSQC spectrum of $E_{133-222}$ could be unambiguously assigned. To identify the region corresponding to the α-helix and β-strands on the secondary structure of the $E_{133-222}$, the deviation of the $^{13}C^{\alpha}$ and $^{13}C^{\beta}$ chemical shifts from random coil values were calculated (Fig. 3b). The ^{13}C chemical shifts of $E_{133-222}$ excluding E134, R158, D195, and the three proline residues at P135, P168, P216 are tabulated in the Table S1 (supplementary data).

Fig. 3 (continued)

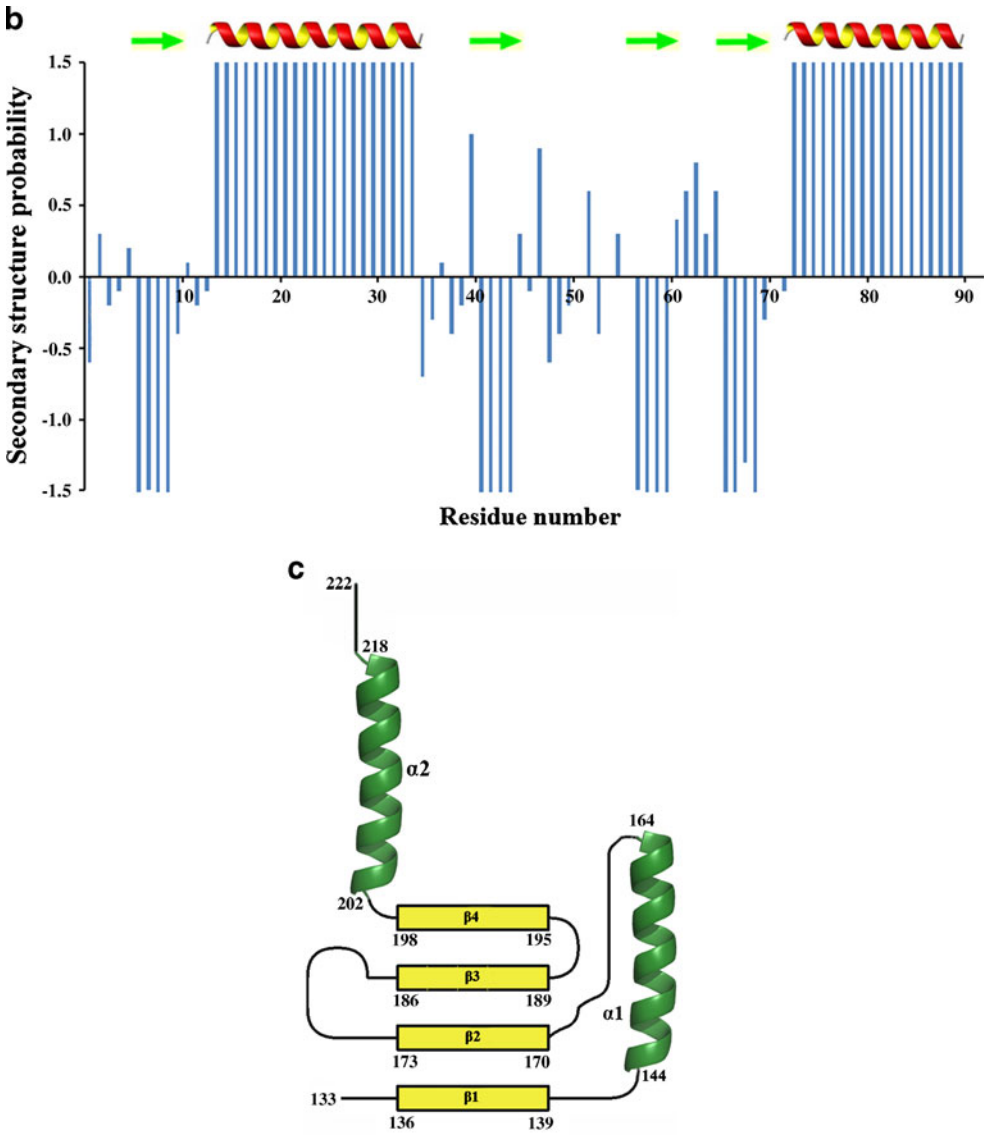

These plotted values illustrate that the protein contains four β-strands and two α-helices in the order of β1:α1:β2:β3:β4:α2. The β-strands consists of four residues including, K136-V139, E170-V173, G186-V189, D195-E198 on each strand, respectively. The helix between the first and the second β-strand comprises of 20 residues from R144-A164 and the helix on the C-terminus of the peptide includes the amino acids T202-I218. A topological model for the arrangements of the α- and β-sheeted region on the domain is given in Fig. 2c. The four β-strands on the C-terminal structure of the subunit E, $E_{133\text{-}222}$, are connected by linker regions with 4–5 amino acids. Together the four β-strands with the α-helical region depict a compact globular domain. The 11 residues at the very C-terminus of subunit E sequence are predicted to be unstructured (McGuffin et al. 2000).

The overall structure of $E_{133\text{-}222}$ is comparable with the C-terminal region of the recently determined crystal structure $E_{101\text{-}206}$ of the related subunit E from the *M. jannaschii* A_1A_O ATP synthase (Balakrishna et al. 2010). A major deviation is due to the arrangement of an additional helix in *M. jannaschii* $E_{101\text{-}206}$. Whereas the V-ATPase $E_{133\text{-}222}$ consists of the secondary features β1:α1:β2:β3:β4:α2, with the residues R144 to A164 forming helix α1, the related helix α1 in $E_{101\text{-}206}$ of the *M. jannaschii* A_1A_O ATP synthase is separated in to a helix α1 and –α2 with the residues K131-D138 and L145-T150, respectively, resulting in the overall secondary elements β1:α1:α2:β2:β3:β4:α3 (Fig. 1).

The structure of the *S. cerevisiae* $E_{133\text{-}222}$ adds insight to the previously described solution NMR structure of $E_{1\text{-}69}$, revealing an extended 83.19 Å long α-helix (Rishikesan

Fig. 4 **a** The arrangements of subunit E, $E_{1\text{-}52}$, (Gayen et al. 2009) and $E_{101\text{-}206}$ (Balakrishna et al. 2010) of the A_1A_O ATP synthase from *M. jannaschii*. The red color mesh region is the uncharacterized region. **b** The arrangements of the *S. cerevisiae* V-ATPase subunit E, $E_{1\text{-}69}$ (Rishikesan et al. 2011) and the presented $E_{133\text{-}222}$ (with green α-helices and yellow β-sheets). The uncharacterized region is shown as a lime green mesh

et al. 2011), and the elongated shape of the entire subunit E, forming together with the recombinant α-helix subunit G (Rishikesan et al. 2011) a rod shaped structure of 180 Å with distinct thick and narrow extremeties (Diepholz et al. 2008). The narrow end consists of the two N-terminal α-helices of subunit G and E, as shown by solution NMR spectroscopy (Rishikesan et al. 2010, 2011). The thick shape of the E-G is described to be contributed by the α-helical C-terminus of subunit G (Rishikesan et al. 2010) and can now be assigned to be composed of the globular C-terminal segment $E_{133\text{-}222}$ with its structural arrangement of β1:α1:β2:β3:β4:α2. Based on these results and

the prediction of the N-terminal tail being a straight helix (Diepholz et al. 2008), we have modeled the NMR structures of $E_{1\text{-}69}$ (Rishikesan et al. 2011) and the presented $E_{133\text{-}222}$, resulting in a crosier-like shape of 180 Å (Fig. 4b). As demonstrated in Fig. 4a, the structure is similar to the one of the homologous subunit E of the A_1A_O ATP synthase (Lee et al. 2010; Balakrishna et al. 2010). Considering the knowledge of a homologous existence, both subunits would share a similar structure and possibly function in the entire complex.

Topological arrangement of *S. cerevisiae* $E_{133\text{-}222}$

Most recently the *M. jannaschii* subunit E was described to bind with its globular C-terminal region $E_{101\text{-}206}$ in the A-B interface at the top of the A_1A_O ATP synthase (Hunke et al. 2011) via the sheets β1 and β2 of subunit E (A168 – I172 and L179 – D183). In parallel, the *M. jannaschii* subunit B interacts with subunit E via the residues R198 and the hydrophobic I201 in the very C-terminal α-helix of E (Hunke, et al. 2011). These residues of $E_{101\text{-}206}$ are located in the similar C-terminal α-helix of the presented V-ATPase domain $E_{133\text{-}222}$, including the conserved residue I218 (Fig. 1). In comparison, cysteine mutagenesis and covalent crosslinking studies in the *S. cerevisiae* V-ATPase have revealed, that subunit E forms crosslink products with the nucleotide-binding subunit B, when the amino acids A15 and K45 at the very top of subunit B have been mutated to cysteins, respectively (Arata et al. 2002). In addition, Flag-tag at the C-terminus of subunit E in electron micrographs of *S. cerevisiae* V_1V_O ATPase supported the localization of the very C-terminal region of E in the neighborhood of the top and thereby the N-terminal region of subunit B (Diepholz et al. 2008). In this context it might be concluded that *S. cerevisiae* V-ATPase subunit E is connected to the top of the A-B headpiece due to the interaction of β1, β2 and the helix α2. This would allow the C-terminal region of E to be hold in the A-B interface like a hinge joint and the extended N-terminal α-helix to be linked together with the N-terminal α-helix of subunit G to the collar-domain of the entire V_1V_O ATPase. Subunit E of the *S. cerevisiae* V_1V_O ATPase has been shown to be an essential component of the reversible V_1 and V_O reassembly (Kane and Smardon 2003), resulting in significant rearrangements of the stalk subunits and bringing the subunits E, G and the central stalk subunit F in close proximity (Grüber 2003) and forming one compact stalk (Svergun et al. 1998; Radermacher et al. 2001; Grüber 2003; Chaban et al. 2005). In this canon the hinge joint would allow subunit E via its C-terminal segment in the process of reversible disassembly of the V_1 and V_O part to alter the arrangement of the more flexible and extended N-terminal α-helix of subunit E. Thereby this rearrangement may move the N-terminus of E in close proximity to the central stalk subunits of V_1 during disassembly, and to the collar-region, when the two sectors assemble to an entire V_1V_O ATPase with two peripheral stalks.

Acknowledgment S. Rishikesan is grateful to the authority of Nanyang Technological University (NTU) for awarding research scholarship. This research was supported by A*STAR BMRC (09/1/22/19/609). We thank Dr. S. Gayen (SBS, NTU) for helpful suggestions concerning NMR data analysis and we are grateful to Dr. M. S. S. Manimekalai (SBS, NTU) for the art work and reading the manuscript.

References

Arata Y, Baleja JD, Forgac M (2002) Biochemistry 41:11301–11307
Armbrüster A, Svergun DI, Coskun Ü, Juliano S, Bailer SM, Grüber G (2004) FEBS Lett 570:119–125
Balakrishna A, Manimekalai MSS, Hunke C, Gayen S, Rössle M, Jeyakanthan J, Grüber G (2010) J Bioenerg Biomembr 42:311–320
Basak S, Gayen S, Thaker YR, Manimekalai MSS, Roessle M, Hunke C, Grüber G (2011) Biochim Biophys Acta - Biomembranes 1808:360–368
Bax A, Freemna R, Kempsell SP (1980) J Magn Reson 41:349–353
Chaban YL, Juliano S, Boekema EJ, Grüber G (2005) Biochim Biophys Acta Biomembr 1708:196–200
Claridge TDW (1999) High-Resolution NMR technique in organic chemistry, edition 1
Diepholz M, Venzke D, Prinz S, Batisse C, Flörchinger B, Rössle M, Svergun DI, Böttcher B, Féthière J (2008) Structure 16:1789–1798
Drory O, Frolow F, Nelson N (2004) EMBO Rep 5:1148–1152
Gayen S, Balakrishna AM, Grüber G (2009) J Bioenerg Biomembr 41:343–348
Grüber G (2003) J Bioenerg Biomembr 35:277–280
Grüber G, Marshanski V (2008) Bioessays 30:1096–1099
Grüber G, Radermacher M, Ruiz T, Godovac-Zimmermann J, Canas B, Kleine-Kohlbrecher D, Huss M, Harvey WR, Wieczorek H (2000) Biochemistry 39:8609–8616
Grüber G, Godovac-Zimmermann J, Link TA, Coskun Ü, Rizzo VF, Betz C, Bailer S (2002) Biochem Biophys Res Comm 298:383–391
Hunke C, Antosch M, Müller V, Grüber G (2011) Biochim Biophys Acta-Biomembranes 1808:2111–2118
Jones RPO, Durose LJ, Findlay JBC, Harrison MA (2005) Biochemistry 44:3933–3941
Kane PM, Smardon AM (2003) J Bioenerg Biomembr 35:313–321
Kneller DG, Goddard TD (1997) SPARKY 3.105. University of California, San Francisco
Laemmli UK (1970) Nature 227:680–685
Lee LK, Stewart AG, Donohoe M, Bernal RA, Stock D (2010) Nat Struct Mol Biol 17:373–378
Marion D, Ikura M, Tschudin R, Bax A (1989) J Magn Reson 85:393–399
Marshansky V, Futai M (2008) Curr Opi Cell Biol 20:415–426
McGuffin L, Bryson K, Jones D (2000) The PSIPRED protein structure prediction server. Bioinformatics 16:404–405

Owegi MA, Carenbauer AL, Wick NM, Brown JF, Terhune KL, Bilbo SA, Weaver RS, Shircliff R, Newcomb N, Parra-Belky KJ (2005) J Biol Chem 280:18393–18402
Radermacher M, Ruiz T, Wieczorek GG (2001) J Struct Biol 135:26–37
Rishikesan S, Gayen S, Thaker YR, Vivekanandan S, Manimekalai MSS, Yau YH, Geifman Shochat S, Grüber G (2009) Biochim Biophys Acta Bioenerg 1787:242–251
Rishikesan S, Manimekalai MSS, Grüber G (2010) Biochim Biophys Acta Biomembr 1798:1961–1968
Rishikesan S, Thaker YR, Grüber G (2011) J Bioenerg Biomembr 43:187–193
Rizzo VF, Coskun U, Radermacher M, Ruiz T, Armbrüster A, Grüber G (2003) J Biol Chem 278:270–275
Sagermann M, Stevens TH, Matthews BW (2001) Proc Natl Acad Sci USA 98:7134–7139
Svergun DI, Konrad S, Huß M, Koch MHJ, Wieczorek H, Altendorf K, Volkov VV, Grüber G (1998) Biochemistry 37:17659–17663
Wilkens S, Vasilyeva E, Forgac M (1999) J Biol Chem 274:31804–31810
Wishardt DS, Sykes BD, Richards FM (1992) Biochemistry 31:1647–1651
Xu T, Vasilyeva E, Forgac M (1999) J Biol Chem 274:28909–28915